

THE UNIVERSITY of EDINBURGH

Edinburgh Research Explorer

Discovery of a low-surface-brightness galaxy in the Zone of Avoidance using VVVX Deepstack imaging

Citation for published version:
Nilo Castellón, JL, Baravalle, L, Minniti, D, Alonso, MV, Galaz, G, Villalon, C, Hinojosa, R, Schmidt, EO, Valotto, C, Soto, M, Rivera, EG, Valdivia-Rojas, V, Alvarez-Rocha, D, Marchant Cortes, P & Cross, NJG 2026, 'Discovery of a low-surface-brightness galaxy in the Zone of Avoidance using VVVX Deepstack imaging', *Astronomy and Astrophysics*, vol. 713, L3, pp. 1-5. https://doi.org/10.1051/0004-6361/202660814

Digital Object Identifier (DOI):
10.1051/0004-6361/202660814

Link:
Link to publication record in Edinburgh Research Explorer

Document Version:
Publisher's PDF, also known as Version of record

Published In:
Astronomy and Astrophysics

General rights
Copyright for the publications made accessible via the Edinburgh Research Explorer is retained by the author(s) and / or other copyright owners and it is a condition of accessing these publications that users recognise and abide by the legal requirements associated with these rights.

Take down policy
The University of Edinburgh has made every reasonable effort to ensure that Edinburgh Research Explorer content complies with UK legislation. If you believe that the public display of this file breaches copyright please contact openaccess@ed.ac.uk providing details, and we will remove access to the work immediately and investigate your claim.

OPEN ACCESS

Download date: 06. Nov. 2026

A&A, 713, L3 (2026)
https://doi.org/10.1051/0004-6361/202660814
© The Authors 2026

Astronomy & Astrophysics

LETTER TO THE EDITOR

Discovery of a low-surface-brightness galaxy in the Zone of Avoidance using VVVX Deepstack imaging

J. L. Nilo-Castellón[1,⋆], L. Baravalle[2,3], D. Minniti[5,6], M. V. Alonso[2,3], G. Galaz[7], C. Villalon[2,3], R. Hinojosa[9], E. O. Schmidt[2,3], C. Valotto[2,3], M. Soto[4], E. G. Rivera[1], V. Valdivia-Rojas[1], D. Alvarez-Rocha[1], P. Marchant Cortés[1], and N. J. G. Cross[8]

[1] Departamento Astronomía, Facultad de Ciencias, Universidad de La Serena, Av. Raul Bitran 1305, La Serena, Chile
[2] Instituto de Astronomía Teórica y Experimental, (IATE-CONICET), Laprida 854, X5000BGR Córdoba, Argentina
[3] Observatorio Astronómico de Córdoba, Universidad Nacional de Córdoba, Laprida 854, X5000BGR Córdoba, Argentina
[4] Instituto de Investigación en Astronomía y Ciencias Planetarias, Universidad de Atacama, Av. Copayapu 485, Copiapó, Chile
[5] Instituto de Astrofísica, Facultad de Ciencias Exactas, Universidad Andrés Bello, Av. Fernandez Concha 700, Las Condes, Santiago, Chile
[6] Vatican Observatory, V00120 Vatican City State, Italy
[7] Instituto de Astrofísica, Pontificia Universidad Católica de Chile, Vicuña Mackenna 4860, 7820436 Macul, Santiago, Chile
[8] Wide-Field Astronomy Unit, Institute for Astronomy, University of Edinburgh, Royal Observatory, Blackford Hill, Edinburgh EH9 3HJ, UK
[9] Cerro Tololo Inter-American Observatory, CTIO/AURA Inc., La Serena, Chile

Received 6 May 2026 / Accepted 7 July 2026

ABSTRACT

We report the discovery of VVVX J080705.96−273823.6, the first low-surface-brightness galaxy candidate identified in the Zone of Avoidance by the VISTA Variables in the Vía Láctea eXtended Survey (VVVX). The source was detected serendipitously during a visual inspection of the new Deepstack images, a set of reconstructed mosaics generated through an updated reprocessing. The associated stacking procedure that significantly improves both the depth and spatial uniformity of the original survey images. First-order morpho-photometric parameters were obtained using `SExtractor` in combination with PSF models derived with `PSFEx`, applied to star-subtracted images to minimize foreground contamination. The final structural properties of the galaxy were derived from PSF-convolved modelling of azimuthally averaged surface-brightness profiles in the J, H, and K_s bands using exponential, Sérsic, and composite models. The galaxy candidate is clearly detected in the three available near-infrared bands. The azimuthally averaged profiles are consistently described by a disk-dominated (exponential) model in all three bands, with exponential scale lengths in the range $h \sim 32$–$36''$ and extinction-corrected central surface brightness values spanning $\mu_0 \simeq 19.82$–22.35 mag arcsec^{-2}. The J band gives the best-constrained profile; H and K_s show the same behaviour with larger uncertainties. The projected proximity to the galaxies ESO 494−25 and ESO 494−26 raises the possibility of a physical association. Both ESO galaxies have radial velocities consistent with distances of ∼11–12 Mpc. If VVVX J080705.96−273823.6 were located at the same distance, its characteristic exponential scale length of $h \simeq 34''$ would correspond to ∼1.8–2.0 kpc, consistent with the range of scale lengths observed in nearby LSB disk galaxies. However, in the absence of a spectroscopic redshift, this association remains tentative. This discovery demonstrates that the new VVVX *Deepstack* products can reveal faint diffuse galaxies at low Galactic latitudes, opening a path toward a more complete census of the obscured nearby Universe.

Key words. surveys – galaxies: irregular – infrared: galaxies

1. Introduction

The Zone of Avoidance (ZoA; Kraan-Korteweg & Lahav 2000) remains the main observational discontinuity in attempts to reconstruct the local cosmic density field. Severe obscuration from the Milky Way, produced by dust extinction, stellar crowding, and diffuse emission (Schlegel et al. 1998; Schlafly & Finkbeiner 2011; Soto et al. 2019), interrupts the continuity of large-scale structure mapping across the Galactic plane. Although extensive multiwavelength surveys over the past decades have identified thousands of previously hidden galaxies behind the Milky Way (e.g., Jarrett et al. 2000; Donley et al. 2005; Henning et al. 2010; Staveley-Smith et al. 2016; Kraan-Korteweg et al. 2018; Baravalle et al. 2018, 2021; Daza-Perilla et al. 2023; Galdeano et al. 2023; Alonso et al. 2025; Baravalle et al. 2026), these efforts have mainly probed the bright end of the luminosity function. Consequently, the faint, diffuse, and low-surface-brightness galaxy population remains poorly constrained. While such systems are not expected to dominate the mass budget individually, their systematic omission can bias the tracer population used to map large-scale structure. In particular, missing faint and diffuse galaxies may lead to an incomplete sampling of structures crossing the Galactic plane, with consequences for dynamical reconstructions, peculiar-velocity fields (Maller et al. 2003), and cosmological inferences based on large-scale structure (Clocchiatti et al. 2024). A more complete census of faint and low-surface-brightness galaxies in the ZoA is therefore required for a physically consistent reconstruction of the local density field.

In this Letter, we report the discovery of VVVX J080705.96−273823.6, the first low-surface-brightness

⋆ Corresponding author: `jnilo@userena.cl`

Open Access article, published by EDP Sciences, under the terms of the Creative Commons Attribution License (https://creativecommons.org/licenses/by/4.0), which permits unrestricted use, distribution, and reproduction in any medium, provided the original work is properly cited.
This article is published in open access under the Subscribe to Open model. Subscribe to A&A to support open access publication.

Table 1. Properties of the PSFEx PSF models.

Filter	N stars	χ^2	FWHM (px)	Ellipticity	Asym.
J	210	0.39	2.72	0.01	0.03
H	276	0.42	2.98	0.01	0.05
K_s	281	0.36	2.51	0.02	0.03

Notes. Columns display the number of stars used to build each PSF model, reduced χ^2 of the fit, FWHM in pixels, ellipticity ($1 - b/a$), and the asymmetry parameter.

galaxy identified in the Zone of Avoidance using data from the VISTA Variables in the Vía Láctea eXtended survey (VVVX). The paper is organized as follows. Sect. 2 describes the data and photometric procedures, Sect. 3 presents the structural characterization, and Sect. 4 summarizes the results and discusses the possible association with nearby galaxies.

2. The data

This work utilizes a new set of deep near-infrared mosaics, hereafter referred to as *Deepstack*, reconstructed from the VISTA Variables in the Vía Láctea eXtended survey (VVVX; Saito et al. 2024). Updated stacking procedures and revised calibrations have been applied to the original VVVX images, producing mosaics with increased depth and improved spatial uniformity[1].

Our analysis focuses on the *Deepstack* images of tile e0778 in the J, H, and K_s bands. The stacks combine 36, 24, and 264 individual frames, yielding total integration times of 1080 s (J), 288 s (H), and 1056 s (K_s). The corresponding 5σ limiting magnitudes for point sources are $J = 20.61$, $H = 19.35$, and $K_s = 18.80$ mag (Vega). All mosaics preserve a pixel scale of $0\farcs34$. We estimated the limiting surface brightness from the sigma-clipped background dispersion in source-free regions of the star-subtracted images, following Román et al. (2020). Over $10'' \times 10''$ areas, we obtained 3σ limits of $\mu_{\rm lim} \simeq 25.6$, 24.3, and 23.6 mag arcsec^{-2} in the J, H, and K_s bands, with the J band being the deepest.

We measured first-order structural parameters with `SExtractor` in a $7' \times 7'$ region centred on VVVX J080705.96−273823.6. To minimize contamination from the dense stellar foreground, while preserving the galaxy's diffuse emission, we adopted a two-pass procedure. In the first pass, `SExtractor` was run with a configuration optimized for compact-source detection, using a Mexican-hat filter, `DETECT_THRESH` = 2, and a large background mesh of `BACK_SIZE` = 192 pixels. The compact sources detected in this pass were used to define a foreground-source mask and to generate a foreground-subtracted image. In the second pass, `SExtractor` was applied to the foreground-subtracted image with a configuration optimized for faint extended emission, using a Gaussian filter, `DETECT_THRESH` = 1, and an area-based selection to isolate the galaxy.

To assess the impact of remaining foreground-subtraction residuals, we measured the residual sky level in source-free elliptical annuli outside the main body of the galaxy. The residual background is consistent with zero, with a region-to-region systematic uncertainty of ∼0.2% of the central intensity. Propagating this systematic through the exponential profile changes μ_0 by $\leq$0.003 mag arcsec^{-2} and h by $\leq$1%. This also affects the outer surface-brightness profile by $\leq$0.02 mag arcsec^{-2} out to $r \sim 80''$. At radii larger than $r \sim 95''$, the profile becomes increasingly affected by subtraction residuals and was therefore excluded from the fit. The adopted fitting range is $6'' < r < 95''$. We therefore conclude that the derived structural parameters are not significantly affected by foreground-subtraction residuals.

The point spread function (PSF) in each band was modelled with PSFEx v3.21.1 (Bertin 2013), using SExtractor detections of point-like sources selected within the stellar locus and with signal-to-noise ratios greater than 10. We adopted empirical pixel-based PSF models on a 25×25 grid. The resulting PSFs yielded full width at half maximum (FWHM) values of 2.72, 2.98, and 2.51 pixels in the J, H, and K_s bands, corresponding to 0.92, 1.01, and 0.85 arcsec, respectively (Table 1).

Following Nilo-Castellón et al. (2025), we verified the photometric calibration through comparison with 2MASS photometry retrieved using `TOPCAT` (Taylor 2011). The 2MASS magnitudes were converted to the VISTA system following Soto et al. (2019). Cross-matching with Gaia DR3 (Gaia Collaboration 2023) within $0\farcs5$ ensured the selection of reliable point sources (`PSS` > 0.99). The resulting median offsets are $\Delta J = 0.02 \pm 0.10$, $\Delta H = 0.05 \pm 0.13$, and $\Delta K_s = 0.07 \pm 0.035$ mag, consistent with the adopted zero-points of 26.2, 25.7, and 24.4 in J, H, and K_s, respectively. All magnitudes were corrected for Galactic extinction following Schlafly & Finkbeiner (2011), adopting $A_J = 0.38$, $A_H = 0.24$, and $A_{K_s} = 0.16$ mag. Given the ∼6′ resolution of the extinction maps, a single value was adopted across the source; we note that residual spatial variations at this low Galactic latitude cannot be excluded.

3. Structural characterization of VVVX J080705.96−273823.6

We detected VVVX J080705.96−273823.6 at $\alpha = 08^{\rm h}07^{\rm m}05\fs96$ and $\delta = -27°38'23\farcs6$ (J2000). In the J-band image, the galaxy is most clearly detected as a diffuse, elongated, and spatially extended system, with its major axis oriented approximately northeast-southwest. The LSB nature of the source is also supported by optical images from the DECaPS2 survey (Saydjari et al. 2023) (Fig. 1). To characterize its structure, we followed a two-step approach: we first used automated source modelling to obtain initial constraints on the size, geometry, and light distribution of the galaxy. We then refined this characterization through a direct modelling of the azimuthally averaged surface-brightness profiles.

First-order structural parameters were obtained with `SExtractor` using `PSFEx` PSF models, following the procedure of Sect. 2. The resulting morpho-photometric parameters are summarized in Table 2, displaying a broadly consistent projected geometry in the J and H bands, with $b/a \sim 0.37$–0.41 ($\epsilon \sim 0.59$–0.63) and PA $\sim 68°$–$70°$. In K_s, the source appears rounder, with $b/a \sim 0.61$ ($\epsilon \sim 0.39$), while maintaining a comparable position angle of PA $\sim 75°$.

The `SExtractor` model-fitting results indicates a strongly disk-dominated structure in the J and K_s bands, while the H-band fit appears less reliable. In the J band, the fitted disk magnitude is very close to the total model magnitude, implying a negligible central spheroidal component at the depth of the data, and the solution is almost entirely disk dominated ($f_{\rm disk} = 0.996$). The K_s band gives a similar result ($f_{\rm disk} = 0.968$). In contrast, the H-band solution yields a much lower disk-to-total flux ratio ($f_{\rm disk} = 0.182$), which is inconsistent with the other bands and likely reflects the lower robustness of the fit, rather than a genuine structural difference. The fitted exponential disk scale

[1] The *Deepstack* images are available through the VISTA Science Archive (VSA; `https://vsa.roe.ac.uk`) for the VVVX team.

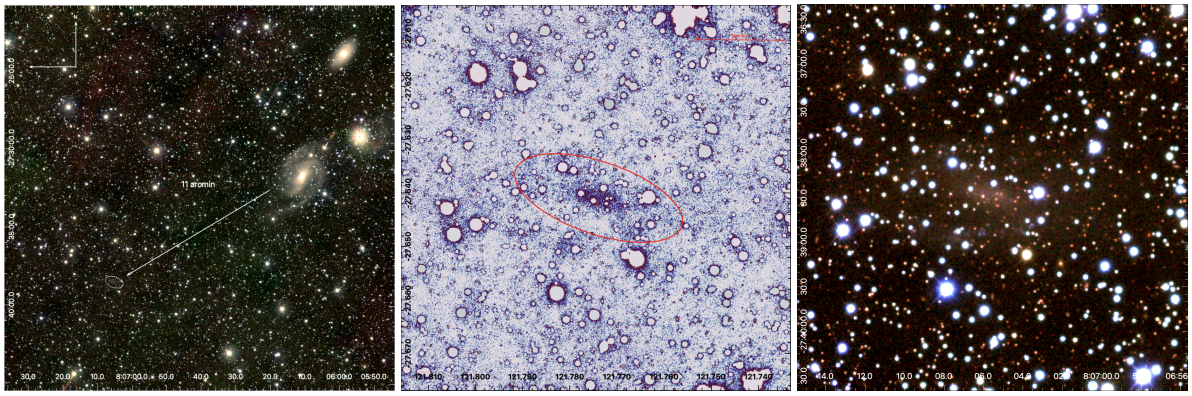


Fig. 1. Left: RGB colour-composite image constructed from a section of the VVVX *Deepstack* J, H, and K_s images tile e0778. The LSB is marked by the dashed ellipse in the lower-left corner 11 arcmin in the southwest direction of the galaxy ESO 494−256. Center: Stellar-subtracted J-band image of VVVX J080705.96−273823.6. The red ellipse marks the `MAG_AUTO` aperture returned by `SExtractor`. Right: RGB colour-composite image constructed from the DECaPS g', r', and i' images. Center and right panels cover a side length of 4.5′.

Table 2. `SExtractor`-based morpho-photometric parameters.

Band	MAG_{AUTO} (mag)	MAG_{disk} (mag)	f_{disk}	h (″)	b/a	PA (°)
J	14.719	14.724	0.996	16.96	0.366	69.61
H	13.100	14.059	0.182	24.35	0.406	68.12
K_s	13.198	13.162	0.968	14.73	0.608	75.02

lengths span $h \sim 14.7''$–$24.4''$. Overall, these results provide a robust first-order description of a flattened, disk-dominated LSB system, with the J band giving the most stable structural constraints for the subsequent surface-brightness analysis.

To obtain quantitative structural parameters, we complemented this automated analysis by modelling the azimuthally averaged surface-brightness profiles directly. We derived the radial light distribution using elliptical apertures on the star-subtracted image. To ensure a consistent comparison between filters, we fixed the profile geometry to the J-band solution (i.e., centroid, axis ratio, and position angle). The mean intensity was measured in concentric annuli of fixed width and converted to surface brightness using the calibration of Sect. 2. To assess the stability of the profile against the background treatment, we measured the residual sky in source-free elliptical annuli well beyond the galaxy ($r \gtrsim 120''$): it is consistent with zero, with a region-to-region systematic of $\simeq$0.08 counts pix^{-1} ($\sim$0.2% of the central intensity). Propagating this systematic through the exponential profile changes μ_0 by $\lesssim$0.003 mag arcsec^{-2} and h by $\lesssim$1% ($\Delta h \lesssim 0.34''$). The outer profile also changes by $\lesssim$0.02 mag arcsec^{-2} out to $r \sim 80''$, which is the radius out to which the profile remains essentially insensitive to the adopted background. Between $r \sim 80''$ and $r \sim 95''$, the residual-sky scatter grows but the profile is still reliably measured, whereas beyond $r \sim 95''$, it becomes increasingly affected by subtraction residuals from neighboring sources.

We fit the profiles with three functional forms: a pure exponential disk, a single Sérsic profile, and a composite exponential+Sérsic model. The fits were performed over the radial interval $6'' < r < 95''$ using weighted least squares, with uncertainties estimated from the dispersion of pixel values within each annulus. Figure 2 shows the observed profiles, the PSF-convolved models, and the corresponding residuals, while the best-fitting structural parameters are summarized in Table 3.

The pure exponential surface-brightness profile fits provide a stable description of the galaxy in all three bands, with scale lengths of $h \sim 32$–$36''$ and extinction-corrected central surface brightnesses of $\mu_0 \simeq 19.82$, 19.81, and 22.35 mag arcsec^{-2} in J, H, and K_s, respectively. The corresponding face-on values are $\mu_{0,\mathrm{face-on}} \simeq 20.91$, 20.91, and 23.44 mag arcsec^{-2}. In the independent `SExtractor`/PSFEx model fits, the low disk-to-total ratio is confined to the H band ($f_{disk} = 0.182$), whereas the J and K_s solutions are both strongly disk-dominated. This behaviour should therefore not be interpreted as a wavelength-dependent trend, but rather as an instability of the automated H-band fit, likely driven by its lower effective depth and/or background structure.

Both approaches support a disk-dominated interpretation, but their scale lengths are not equivalent measurements. The `SExtractor`/PSFEx values are first-order estimates from automated model fitting, sensitive to segmentation, detection threshold, masking, background treatment, PSF model, and the effective radial extent of the detected light. The direct profile fits explicitly model the azimuthally averaged exponential over the adopted radial range, and their systematically longer scale lengths reflect the more complete treatment of the low-surface-brightness outskirts. Therefore, we used the `SExtractor`/PSFEx results as a morphological consistency check and adopted the profile-fit values of $h \sim 32$–$36''$ as the fiducial disk scale lengths.

4. Summary and conclusions

We report the discovery of VVVX J080705.96−273823.6, a low-surface-brightness (LSB) galaxy identified behind the Milky Way using the new VVVX *Deepstack* images. The source is located at $\alpha = 08^h07^m05^s.96$ and $\delta = -27°38'23''.6$ (J2000) and appears as a diffuse and extended system detected in the near-infrared J, H, and K_s images.

Our analysis followed a two-step approach. First, automated modelling with `SExtractor` indicated disk-dominated solutions in the J and K_s bands ($f_{disk} = 0.996$ and 0.968), with a less stable H-band fit ($f_{disk} = 0.182$) likely affected by the lower effective depth of the image. The exponential model gives stable scale lengths across the three bands ($h \sim 32$–$36''$) and extinction-corrected central surface brightnesses of $\mu_0 \simeq 19.82$, 19.81, and 22.35 mag arcsec^{-2} in J, H, and K_s, supporting an extended disk-like system.

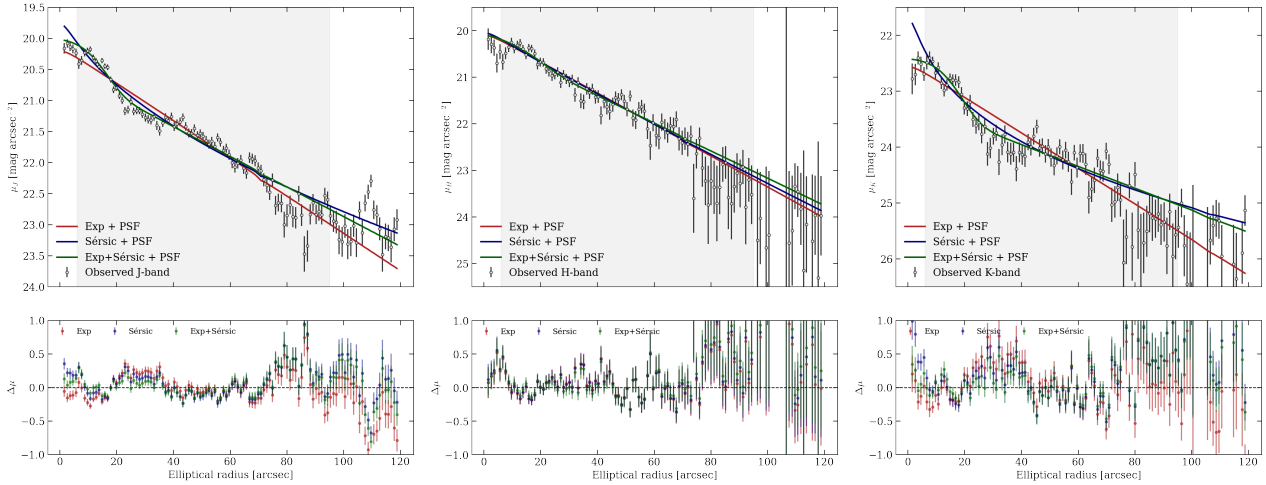


Fig. 2. Azimuthally averaged surface-brightness profiles of VVVX J080705.96−273823.6 in the J, H, and K_s bands. Top: Observed profiles (black circles) and PSF-convolved exponential (red), Sérsic (blue), and exponential+Sérsic (green) models. Shaded regions indicate the fitted radial ranges. Bottom: Residuals for each model.

Table 3. Best-fit parameters of the exponential disk model.

Band	μ_0	h	$\mu_{0,\mathrm{face-on}}$
J	19.819 ± 0.015	36.053 ± 0.433	20.912
H	19.813 ± 0.031	32.443 ± 0.811	20.905
K_s	22.348 ± 0.032	34.178 ± 0.846	23.440

Notes. PSF-convolved fits to the azimuthally averaged surface-brightness profiles. Surface brightnesses are corrected for Galactic extinction following Schlafly & Finkbeiner (2011). Sérsic and composite-model fits are given in Appendix A.

The projected proximity of VVVX J080705.96−273823.6 to the nearby galaxies ESO 494−25 and ESO 494−26, located at an angular separation of ∼11′, raises the possibility of a physical association. Both ESO galaxies have radial velocities consistent with distances of ∼11–12 Mpc. If VVVX J080705.96−273823.6 were located at the same distance, its characteristic exponential scale length of $h \simeq 34''$ would correspond to ∼1.8–2.0 kpc, consistent with the range of scale lengths observed in nearby LSB disk galaxies (Galaz et al. 2002). However, in the absence of a spectroscopic redshift, this association remains tentative. Confirming or ruling out a physical connection with the nearby ESO galaxies will require spectroscopic follow-up.

Taken together, the resolved low-surface-brightness morphology, large exponential scale lengths, independent optical confirmation in DECaPS, and central surface brightnesses (consistent with those of nearby LSB disk galaxies) support a coherent interpretation in which VVVX J080705.96−273823.6 is a low-surface-brightness disk galaxy dominated by an extended diffuse component. More broadly, the discovery demonstrates that the new VVVX *Deepstack* products have the capacity to reveal faint diffuse galaxies even in highly obscured regions of the Zone of Avoidance, opening a practical route toward a more complete census of hidden extragalactic structures behind the Milky Way.

Acknowledgements. J.L.N-C. is grateful to the Universidad de La Serena for providing the academic environment and institutional support that enabled the development of this research. L.D.B., M.V.A. and C.V. thank the support of the Consejo de Investigaciones Científicas y Técnicas (CONICET) and Secretaría de Ciencia y Técnica de la Universidad Nacional de Córdoba (SeCyT). D.M. and G.G. acknowledge support from CATA through ANID BASAL FB210003; D.M. also acknowledges Fondecyt Project No. 1220724 and ANID BASAL ACE210002. M.S. acknowledges support from ANID's FONDECYT Regular grant No. 1251401. We gratefully acknowledge the use of data from the ESO Public Survey program IDs 179.B-2002 and 198.B2004 obtained with the VISTA telescope, and optical data products from the Cambridge Astronomical Survey Unit (CASU), the University of Edinburgh Wide Field Astronomy Unit (WFAU), who are responsible for the VISTA Science Archive (VSA). VVV and VVVX data are published in the ESO Science Archive in the data collections identified by the following DOIs: https://doi.eso.org/10.18727/archive/67 and https://doi.eso.org/10.18727/archive/68. We acknowledge Mike Read for his contribution to the quality control of the VVVX DeepStack images, and Eckhard Sutorius for his major role in the production of the DeepStack products used in this work.

References

Alonso, M. V., Baravalle, L. D., Nilo-Castellón, J. L., et al. 2025, A&A, 700, A33
Baravalle, L. D., Alonso, M. V., Nilo Castellón, J. L., Beamín, J. C., & Minniti, D. 2018, AJ, 155, 46
Baravalle, L. D., Alonso, M. V., Minniti, D., et al. 2021, MNRAS, 502, 601
Baravalle, L. D., O'Mill, A. L., Alonso, M. V., et al. 2026, A&A, 705, A242
Bertin, E. 2013, Astrophysics Source Code Library [record ascl:1301.001]
Clocchiatti, A., Rodríguez, Ó., Órdenes Morales, A., et al. 2024, ApJ, 971, 19
Daza-Perilla, I. V., Sgró, M. A., Baravalle, L. D., et al. 2023, MNRAS, 524, 678
Donley, J. L., Staveley-Smith, L., Kraan-Korteweg, R. C., et al. 2005, AJ, 129, 220
Gaia Collaboration (Vallenari, A., et al.) 2023, A&A, 674, A1
Galaz, G., Dalcanton, J. J., Infante, L., & Treister, E. 2002, AJ, 124, 1360
Galdeano, D., Ferrero, G. A., Coldwell, G., et al. 2023, A&A, 669, A7
Henning, P. A., Springob, C. M., Minchin, R. F., et al. 2010, AJ, 139, 2130
Jarrett, T. H., Chester, T., Cutri, R., & Schneider, S. 2000, AJ, 120, 298
Kraan-Korteweg, R. C., & Lahav, O. 2000, A&ARv, 10, 211
Kraan-Korteweg, R. C., van Driel, W., Schröder, A. C., Ramatsoku, M., & Henning, P. A. 2018, MNRAS, 481, 1262
Maller, A. H., McIntosh, D. H., Katz, N., & Weinberg, M. D. 2003, ApJ, 598, L1
Nilo-Castellón, J. L., Alonso, M. V., Baravalle, L. D., et al. 2025, A&A, 704, A209
Román, J., Trujillo, I., & Montes, M. 2020, A&A, 644, A42
Saito, R. K., Hempel, M., Alonso-García, J., et al. 2024, A&A, 689, A148
Saydjari, A. K., Schlafly, E. F., Lang, D., et al. 2023, ApJS, 264, 28
Schlafly, E. F., & Finkbeiner, D. P. 2011, ApJ, 737, 103
Schlegel, D. J., Finkbeiner, D. P., & Davis, M. 1998, ApJ, 500, 525
Soto, M., Barbá, R., Minniti, D., et al. 2019, MNRAS, 488, 2650
Staveley-Smith, L., Kraan-Korteweg, R. C., Schröder, A. C., et al. 2016, AJ, 151, 52
Taylor, M. 2011, Astrophysics Source Code Library [record ascl:1101.010]

Appendix A: Additional structural models and PSF properties

Table A.1. Sérsic and composite exponential+Sérsic PSF-convolved fits. Surface brightnesses (mag arcsec^{-2}) are corrected for Galactic extinction; scale parameters in arcsec.

Sérsic + PSF						
Band	μ_e	r_e	n	$\mu_{0,\mathrm{infer}}$	$\mu_{0,\mathrm{face-on}}$	AIC
J	22.615 ± 0.154	107.134 ± 10.445	1.821 ± 0.127	19.016	20.109	390.7
H	21.715 ± 0.121	56.834 ± 3.905	1.075 ± 0.099	19.738	20.830	114.5
K_s	26.883 ± 0.956	300.000 ± 186.941	3.295 ± 0.798	20.086	21.179	184.5
Exponential + Sérsic + PSF						
Band	$\mu_{0,\mathrm{disk}}$	h	$\mu_{e,\mathrm{S}}$	$r_{e,\mathrm{S}}$	n_S	AIC
J	20.159 ± 0.034	45.212 ± 1.210	21.089 ± 0.082	11.128 ± 0.541	0.300	266.6
H	20.029 ± 0.108	36.910 ± 2.523	22.115 ± 0.330	14.207 ± 2.887	0.300	108.8
K_s	23.046 ± 0.095	55.642 ± 4.865	23.294 ± 0.108	12.364 ± 0.841	0.300	151.1